Advance View
https://doi.org/10.3354/meps12838

MARINE ECOLOGY PROGRESS SERIES
Mar Ecol Prog Ser

Available online:
February 1, 2019

Contribution to the Theme Section 'Drivers of dynamics of small pelagic fish resources: biology, management and human factors'

Understanding the 3D environment of pelagic predators from multidisciplinary oceanographic surveys to advance ecosystem-based monitoring

Maite Louzao[1,2,*], Isabel García-Barón[1], Anna Rubio[1], Udane Martínez[1], José Antonio Vázquez[3], José Luis Murcia[4], Enrique Nogueira[5], Guillermo Boyra[1]

[1]AZTI, Herrera kaia, Portualdea z/g, 20110 Pasaia, Spain
[2]Centro Oceanográfico de Xixón, Instituto Español de Oceanografía, Avda. Príncipe de Asturias 70 bis, 33212 Xixón, Spain
[3]Alnilam Research and Conservation Ltd., Pradillos 29, 28491 Navacerrada, Madrid, Spain
[4]Asociación de Naturalistas del Sureste (ANSE), Plaza Pintor José María Párraga 11, Bajo, 30002 Murcia, Spain
[5]Instituto Español de Oceanografía, CO de Vigo, Subida al Radio Faro 50-52, 36390 Vigo, Spain

ABSTRACT: Marine predators move through the seascape searching for foraging resources. Prey configuration and oceanographic processes could therefore shape their 3-dimensional (3D) oceanographic habitats. Taking advantage of multidisciplinary oceanographic surveys targeting biomass estimation of pelagic fishes (i.e. JUVENA surveys), observations of 2 highly migratory pelagic seabirds were collected during line-transects: sooty shearwaters (SOSHs) *Ardenna grisea* and great shearwater (GRSHs) *A. gravis*. Every autumn these species visit the pelagic ecosystem of the Bay of Biscay (BoB). We developed generalised additive models to disentangle the effects of the 3D ocean environment and preyscapes at different depth ranges, in addition to static variables, on driving the spatial abundance of these predators. The species differed in their vertical habitat use, with SOSHs and GRSHs influenced by habitat conditions above the depth of the maximum temperature gradient and at the surface, respectively. SOSHs were more abundant in deeper shelf areas with localised hotspots associated with upwelling and river discharges. In contrast, GRSHs were more abundant in shallow slope areas in the outer BoB sectors, followed by less dense areas with intermediate levels of juvenile anchovy biomass. Therefore, both species integrate marine resources at different vertical and spatial dimensions, influenced by topographic features, oceanographic conditions and preyscapes. Relative abundance estimations provided mean values of 3203 SOSHs (95% CI: 1753–5748) and 12 380 GRSHs (95% CI: 5797–28152) in the BoB during their annual migration; these numbers varied slightly inter-annually. This study provides an example of the combination of multiple pelagic components as a means to provide an integral assessment to advance ecosystem-based monitoring.

KEY WORDS: Highly migratory predators · Multidisciplinary oceanographic surveys · Small pelagic fish · Physical oceanography · Generalised additive models · Bay of Biscay

1. INTRODUCTION

Marine predators move through the seascape searching for prey that vary spatially across different water masses/regions and vertically through the water column. During migration, predators make stopovers in certain marine regions to refill their energetic reserves in order to complete their annual migratory journey (Stenhouse et al. 2012). These marine regions are frequently characterized by productive waters, where the vertical and horizontal distribution of prey resources is governed by diverse oceanographic processes, and which can be visited recurrently year after year (Block et al. 2011, Nur et al. 2011, Louzao et al.

*Corresponding author: maite.louzao@gmail.com

2015). Therefore, prey configuration and oceanographic processes may shape the 3-dimensional (3D) oceanographic habitats of highly migratory predators, which can be very predictable (Block et al. 2011). The effect of fisheries on the availability of prey for top predators is a long-standing issue (Cury et al. 2011, Bertrand et al. 2012, Sydeman et al. 2017) and critical foraging grounds should be identified to advance their conservation and management to potentially secure prey availability in these areas (Boyd et al. 2015). When critical areas of highly migratory predators are persistent over time the implementation of spatially-explicit conservation initiatives is more feasible (Lascelles et al. 2014).

The Bay of Biscay (hereafter BoB) represents an important non-breeding foraging ground for numerous predators during certain periods of the year (Fossette et al. 2010, Lezama-Ochoa et al. 2010, Doherty et al. 2017, Lambert et al. 2017, Pérez-Roda et al. 2017, García-Barón et al. 2019). The seabird population of the BoB is highly diverse due to the visits of different trans-equatorial migrating species (Stenhouse et al. 2012, Louzao et al. 2015). Moreover, the BoB represents both a major flyway for north European breeding seabirds during migration periods and an important wintering ground (Arcos et al. 2009, Fort et al. 2012, Pettex et al. 2017). In this biogeographic area, there is evidence that the spatiotemporal distribution of some fish predators (e.g. albacore tuna *Thunnus alalunga*) is driven by early stages (corresponding to young-of-the-year) of the European anchovy *Engraulis encrasicolus* (Lezama-Ochoa et al. 2010). However, there is no evidence whether other pelagic predators, such as seabirds, exploit similar foraging resources and, therefore, whether their oceanographic habitats could be shaped by early stages (juveniles) of different fish species. The importance of early stages of fish as prey for seabirds has been largely evidenced in other geographic areas such as the North Sea (Daunt et al. 2008), the Barents Sea (Barrett 2002) and the Bering Sea (Hatch & Sanger 1992), among others. In the BoB, few studies have related the distribution and abundance of marine predators to that of their prey (but see Certain et al. 2011), given the difficulty in obtaining simultaneous data on both prey and predator distributions. In addition, the relatively low number of seabird breeding colonies in the BoB hinders the study of their foraging ecology.

Annual multidisciplinary oceanographic surveys directed to assessing the stock of commercial pelagic resources provide an ideal platform to simultaneously monitor annual changes of different components of the pelagic ecosystem (Irigoien et al. 2009, Certain et al. 2011, Santos et al. 2013, Authier et al. 2018). In the BoB, the JUVENA oceanographic survey is conducted every year in late summer, and has collected concurrent information on pelagic fishes since 2003 (Boyra et al. 2013) and on plankton and marine megafauna observations since 2012 (García-Barón et al. 2019). These surveys provide information on inter-annual variation in the patterns of spatial distribution and biomass of small pelagic fish (Boyra et al. 2013) as indicators of food availability for pelagic predators (Lezama-Ochoa et al. 2010). Surveys specifically dedicated to the estimation of predator abundance need to cover large areas within the distribution range of predators (e.g. Hammond et al. 2013, Pettex et al. 2017), so are rarely run on an annual basis. In contrast, annual monitoring surveys cover smaller areas (e.g. regions), but at higher frequency. Therefore, large spatial coverage surveys conducted at a lower frequency and regional coverage surveys conducted every year provide complementary approaches (Saavedra et al. 2018).

One of the main advantages of multidisciplinary surveys is the possibility of considering the joint effect of the 3D preyscapes and ocean dynamic environments on driving abundance patterns of highly migratory seabirds. Prey availability depends on abundance, predictability, degree of aggregation, accessibility and depth range (Regular et al. 2013, Thaxter et al. 2013, Boyd et al. 2015). For air-breathing predators such as seabirds, prey availability at shallow depths is particularly important in identifying important foraging grounds (Boyd et al. 2015), since seabirds might be limited by their maximum diving depth. Most studies assessing their oceanographic habitats have been based on surface oceanographic conditions and integrating the vertical range of prey (Boyd et al. 2015), but sub-surface oceanographic processes can be crucial in understanding seabird distribution patterns (Scott et al. 2010). Defining biologically meaningful depth ranges (e.g. considering prey accessibility) to describe 3D preyscape and oceanography can be a critical step in understanding seabird abundance patterns (Thackeray et al. 2010, Cox et al. 2013).

Two highly migratory seabird species, the sooty shearwater (SOSH) *Ardenna grisea* and the great shearwater (GRSH) *A. gravis*, visit the BoB during the autumn during their annual migratory journey. Both species reproduce on remote islands of the South Atlantic Ocean and migrate to the North Atlantic Ocean during the non-breeding period. Millions of individuals visit the productive Northwestern

Atlantic waters from June to August (Hedd et al. 2012). Afterwards, they cross to the eastern North Atlantic following prevailing wind patterns at middle latitudes (Hedd et al. 2012). Breeding individuals will continue their migratory journey to their breeding quarters, but many non-breeding individuals will arrive at the BoB between August and October (Hobbs et al. 2003). Their stopover in the BoB depends on climate variability at long timescales (i.e. North Atlantic Oscillation), adjusted by optimal flying conditions and foraging grounds during migration (Louzao et al. 2015). Both species shape their arrival at the BoB by periods of potential minimum flying costs (Louzao et al. 2015). There is a lack of knowledge of pelagic seabird movements and the oceanographic processes driving their abundance at potentially important stopovers such as the BoB.

Within this context, we aimed at understanding the pelagic seabird 3D environment from multidisciplinary oceanographic surveys. Specifically, our objectives were to assess the importance of (1) prey fields (preyscapes) and (2) mesoscale oceanographic features in driving SOSH and GRSH abundance patterns, with the ultimate aim of (3) obtaining spatial abundance predictions of these highly pelagic predator species in the BoB. We developed generalised additive models (GAMs) to disentangle the effect of the 3D preyscape, 3D ocean dynamic environment, 2D oceanographic predictors and static variables on driving the spatial abundance patterns of these highly migratory predators. We validated the development of 3D predictors that integrate the outputs of ecosystem-based surveys by identifying the biologically meaningful depth ranges linked to the ecology of the predators.

2. MATERIALS AND METHODS

2.1. Multidisciplinary surveys

JUVENA surveys cover the shelf-slope areas of the BoB every September (Fig. 1). The sampling strategy is designed to monitor European anchovy and other small pelagic fish over both Spanish and French continental shelf and slope waters (Boyra et al. 2013). The semi-adaptive sampling scheme is based on across-shelf transect lines from the coast (20 m bottom depth) to beyond the shelf break. Transects are parallel, regularly spaced and perpendicular to the coast with an inter-transect distance of 15 nautical miles (nmi) (Boyra et al. 2013). The offshore and along-coast extension of transects are conditioned by the distribution of the European anchovy positive area encountered. Two vessels (R/V 'Ramón Margalef' and R/V 'Emma Bardán', hereafter R/V RM and R/V EB, respectively) are used simultaneously to cover the extensive area potentially occupied by the European anchovy.

2.1.1. Seabird observations

Line-transect surveys were conducted every September between 2013 and 2016 by a team of 3 experienced observers (2 at a time), who were placed at a height of 7.5 m on board R/V RM. At the beginning of each observation period, observers recorded the meteorological and sea-state conditions that could affect sightings (i.e. wind speed and direction, Beaufort sea-state [a categorical scale that relates wind speed to observed conditions at sea], swell height, glare intensity and visibility). The port observer scanned the water to the front of the boat covering the area from 270–10° on the port side and the starboard observer from 350–90° on the starboard side. In this way, the transect line was well covered while the vessel was navigating at a constant heading and speed during daytime. Observations were performed with the naked eye, while the identification of species and the number of individuals was aided by 10 × 42 Swarovski binoculars. For each observation, the radial distance to bird clusters (individual birds or groups of birds of the same species; Ronconi & Burger 2009) and the angle of the cluster sighting with respect to the track-line at first detection were estimated. Distance was recorded using a stick based on the Heinemann (1981) method and the angle based on an angle meter. Additional data collected from each sighting included species, group size (i.e. number of birds), movement direction, behaviour, etc. Observation effort was located geographically based on the vessel GPS, which logged geographic coordinates every 1 min.

2.1.2. 3D preyscapes

Pelagic fish represent 37 and 46% of the average diet of SOSHs and GRSHs during the non-breeding season, respectively (Ronconi et al. 2010a) (Table S1.1 in Supplement 1 at www.int-res.com/articles/suppl/m12838_supp.pdf [link for all supplements]). Therefore, we obtained 3D spatial biomass patterns of juvenile and adult European anchovy (hereafter as ANEJ and ANEA, respectively) and European pil-

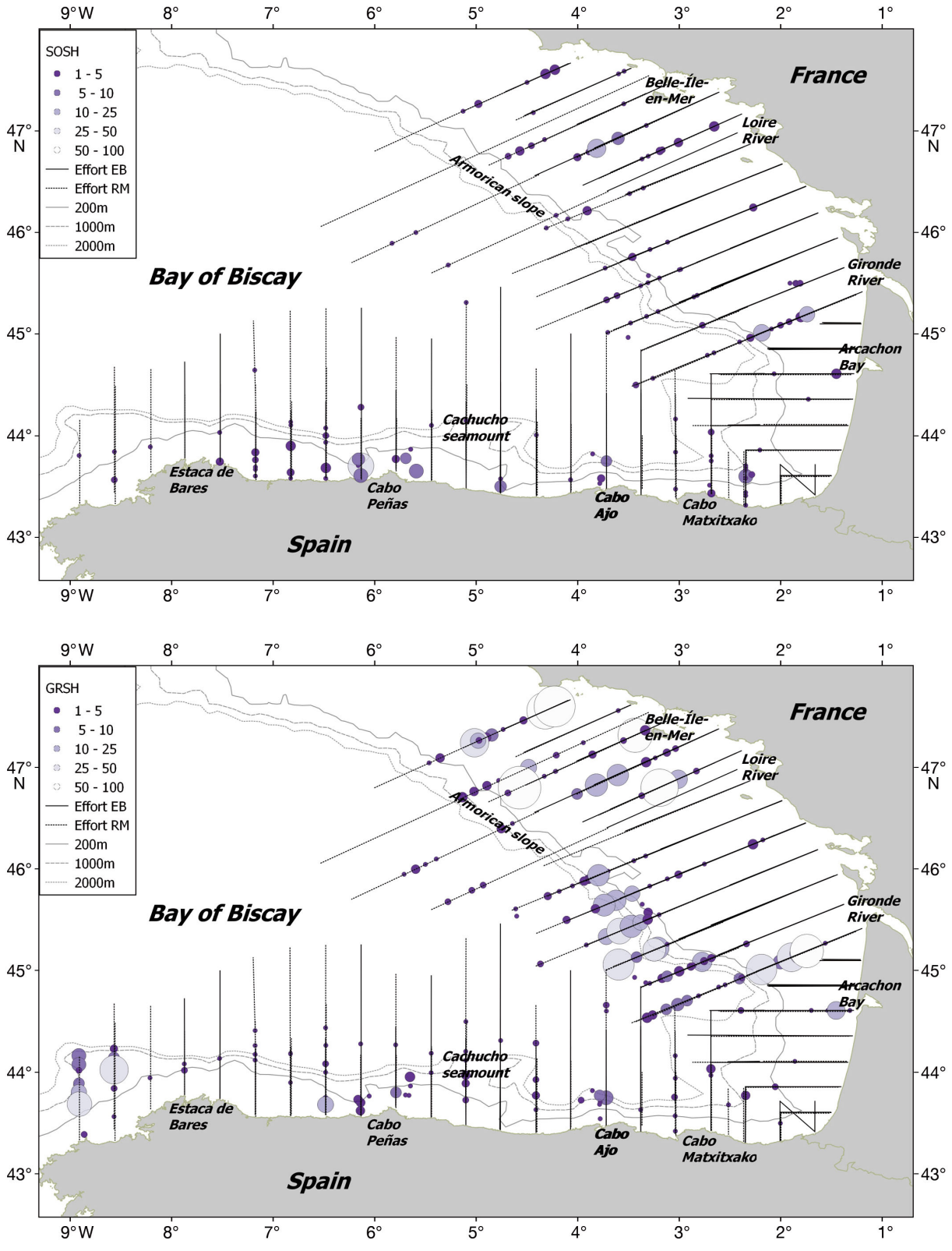

Fig. 1. Sooty shearwater (SOSH) and great shearwater (GRSH) observations during the JUVENA surveys. Circle sizes are proportional to the group size. Survey effort is represented separately for the 2 oceanographic research vessels (EB: 'Emma Bardán'; RM: 'Ramón Margalef'). Isobaths of 200 m (i.e. representing the shelf-break), 1000 m and 2000 m are indicated. Geographical references mentioned in the text are shown

chard (hereafter as PIL) from both R/V RM and R/V EB, based on trawl-acoustic methodology (Simmonds & MacLennan 2005). Data on similar prey species have been used to model shearwater abundance in other temperate latitudes (Phillips et al. 2017). The acoustic equipment included Simrad EK60 split-beam echosounders (Kongsberg Simrad) of 38, 120 and 200 kHz (Boyra et al. 2013). Catches from the fishing hauls and echo-trace characteristics were used to identify fish species and to determine the population size structure. The location of the trawls was selected based on the aggregation structure of the echograms: each time the fish aggregations changed, the acoustic sampling and observations were interrupted to make a trawl. Afterwards, echograms were examined visually with the aid of the species composition of the catch.

For estimation of spatial abundance patterns, the 38 kHz acoustic data were processed by layer echo integration with the Movies+ software (Ifremer), using an elementary sampling distance unit of 0.1 nmi. Echoes were thresholded to −60 dB and integrated into appropriate depth layers (of ~10–50 m depth; and of ~50 m below that depth). More details related to pelagic prey abundance estimation is given in Boyra et al. (2013).

Depths down to 200 m were sampled in 2013 and 2014, and down to 300 m in 2015 and 2016, and the different depth intervals were integrated. The 200 m range limit is typical of small pelagic acoustic surveys and is assumed to contain 100% of the European anchovy and European pilchard biomass (e.g. Massé 1996, Petitgas et al. 2006, Boyra et al. 2013, 2016). Thus, the increase of depth limit to 300 m after 2015 (changed to include information of some mesopelagic species not considered in this work) should not have introduced any bias for the prey species considered here.

Original biomass values (in tonnes) per 0.1 nmi were laid over a standard grid in the study area (latitudinal range: 43.2–47.7° N; longitudinal range: 1.3–7.7° W) consisting of a regular grid with a cell size of 0.1 × 0.1° (see Fig. 2). Original biomasses corresponding to each cell were totalled. A combination of universal kriging and an automatic variogram fitting procedure was applied to obtain small pelagic fish biomass estimations based on the 'automap' package in R (Hiemstra et al. 2009).

2.1.3. 3D oceanographic seascapes

Here, we focused on mesoscale oceanography (referring to physical processes of spatial scales between ~10 and ~100 km and timescales from several days up to 1 mo) since these are the scales that can be solved using physical data gathered during the JUVENA surveys. We used 2D and 3D descriptors to characterise the oceanographic habitat of seabirds (Table 1). The 3D oceanographic predictors were temperature (TEM; °C), salinity (SAL; psu) and geostrophic velocity (GEO; m s^{-1}), whereas the 2D oceanographic predictors corresponded to depth of maximum temperature gradient (DTG; m), maximum

Table 1. Predictors obtained from annual JUVENA oceanographic surveys and additional static variables. Sea surface temperature gradient is derived from interpolated temperature fields at 10 m depth (i.e. temperature at the shallowest depth; TEM_{10})

Predictor	Acronym	Dimensions	Source
Preyscapes			
Biomass of juveniles of European anchovy (tonnes)	ANEJ	3D	Acoustic and pelagic trawls
Biomass of adults of European anchovy (tonnes)	ANEA	3D	Acoustic and pelagic trawls
Biomass of European pilchard (tonnes)	PIL	3D	Acoustic and pelagic trawls
Ocean dynamic environment			
Salinity (psu)	SAL	3D	CTD casts
Temperature (°C)	TEM	3D	CTD casts
Geostrophic velocity (m s^{-1})	GEO	3D	CTD casts
Depth of maximum temperature gradient (m)	DTG	2D	CTD casts
Maximum temperature gradient (°C m^{-1})	MTG	2D	CTD casts
Sea surface temperature gradient	SSTG	2D	Derived from TEM_{10}
Static variables			
Bathymetry (m)	BAT	2D	ETOPO 1
Bathymetric spatial gradient	BATG	2D	Derived from ETOPO 1
Distance to shelf-break (km)	DSB	2D	Derived from Coastline Extractor
Distance to coast (km)	DCO	2D	Derived from Coastline Extractor

temperature gradient (MTG; °C m^{-1}) and sea surface temperature gradient (SSTG).

CTD casts (using a SBE25 and a SBE911 on the R/V EB and RM, respectively) were used to obtain vertical depth profiles of TEM and SAL at selected stations along transects. Based on these vertical profiles, density values (or specific volume) were obtained and integrated over depth to obtain the dynamic height (DYN). Based on Rubio et al. (2009), DYN was computed relative to the next vertical level and not to a common reference level. Once DYN was interpolated over the study area, GEO values were obtained (further methodological details below).

To characterise water column stability, we estimated DTG, computed by adjusting the vertical profiles of TEM to a logistic function (following methodology used in Caballero et al. 2016). The inflexion point of the logistic function (determined using the maximum of its first derivative) marks out the mean depth of the most intense gradient within the thermocline. MTG was obtained using linear differences in the points adjacent to the DTG, which is an indicator of the strength of the water column stratification.

To obtain horizontal fields of TEM, SAL, DYN, DTG and MTG, we used the optimal statistical interpolation (OSI) scheme described in Gomis et al. (2001) in a regular 33 × 54 grid, covering all the study area with regular node distances of 0.15 × 0.15° (further methodological details in Supplement 2).

From DYN interpolated fields, GEO was obtained by the first derivative between adjacent grid nodes. To obtain 3D matrix fields, horizontal analyses were performed independently at 5 dbar intervals (except for DTG and MTG, which are 2D fields) from 10 to 200 m (below this level, the information available was poor and did not allow obtaining consistent horizontal fields). The horizontal interpolated fields of all the variables were finally re-sampled with the 'raster' package (Hijmans & van Etten 2014) to match the standard grid.

Furthermore, we considered an additional variable to describe horizontal TEM changes as a coarse indicator of the presence of oceanographic fronts (Table 1). The shallowest TEM interpolated field was used to derive the spatial gradient of sea surface temperature (SSTG) by means of a spatial moving window within an area of 3 × 3 cells (0.3 × 0.3°). This 2D predictor has previously been identified as an important variable to explain seabird distribution patterns (Louzao et al. 2009). More details about the computation of spatial gradients appear in the following section.

2.1.4. Static variables

Four different static variables were obtained to define seabird oceanographic habitats: bathymetry (BAT; m) and its spatial gradient (BATG; dimensionless), distance to the coastline (DCO; km) and distance to the shelf break (DSB; km) (Table 1 & Fig. S3.1). Bathymetry was obtained from the topographic data ETOPO1 at 0.016° after removing the land topographic data (http://coastwatch.pfeg.noaa.gov/erddap/griddap/etopo180.html) (Amante & Eakins 2009). The coastline was obtained from the Coastline Extractor hosted by the NOAA/National Geophysical Data Center (www.ngdc.noaa.gov/mgg_shorelines/).

Static variables were obtained at the spatial scale of the standard grid. Original bathymetric data were overlaid over the standard grid; those values occurring in the same cell size were averaged. Then, a spatial moving window was used to estimate the spatial differences in bathymetric values (i.e. bathymetric spatial gradient [SG]) within an area of 3 × 3 cells (0.3 × 0.3°) as follows:

$$SG = \frac{\text{maximum value} - \text{minimum value}}{\text{maximum value}} \times 100$$

This dimensionless metric expresses the magnitude of change in bathymetric values, scaled to the maximum value (Louzao et al. 2006). An increased variation in the depth in offshore waters (higher bathymetric gradients in slope areas; Fig. S3.1b) can be considered a proxy of the areas where internal waves generate (Scott et al. 2010). In addition to a steep sea-floor slope, strong barotropic tidal forcing and strong stratification gradients are needed for enhanced internal tide formation. In the BoB, maximum internal tide ranges are located over the Armorican slope, where the barotropic tidal forcing is very energetic (Serpette & Mazé 1989, Le Cann 1990, Pairaud et al. 2010).

The distances between the centre of each cell and both DCO and DSB (i.e. defined by the isobath of 200 m depth) were estimated based on the 'fields' package (Nychka et al. 2017).

2.2. Characterising the vertical domain

To consider the 3D pelagic environment, we adapted the collected biological and physical information to 3 different depth criteria: (1) surface conditions and integrated conditions limited by (2) the diving capability of the deep diver SOSH and (3) the accessibility of pelagic prey. In the first case,

the depth range was set by the shallowest depth layer available in the data set considered, which matches with the diving capabilities of the GRSH (maximum diving depth of 18.9 m; Ronconi et al. 2010b). In the second, the depth limit was set at 70 m given the maximum diving depth of the SOSH (Shaffer et al. 2009), which has been similarly applied in previous work (Phillips et al. 2017). In the third case, the vertical depth was limited by DTG, as the main potential prey (ANEJ) are commonly found above the thermocline (above 50 m depth) (Boyra et al. 2013, 2016). In this way, we summarised oceanographic and preyscape data considering the vertical structure of the water column.

To accommodate ecological predictors of the different vertical criteria, preyscapes were represented by the shallowest biomass between 5 and 15 m depth (indicated by $ANEJ_{10}$, $ANEA_{10}$ and PIL_{10}), the sum of biomass from 5 to 70 m depth (indicated by $ANEJ_{70}$, $ANEA_{70}$ and PIL_{70}) or the sum of biomass from the surface up to the DTG estimated for each cell and year (indicated by $ANEJ_{DTG,}$ $ANEA_{DTG}$ and PIL_{DTG}). Similarly, oceanographic conditions were described by the shallowest depth (10 m; indicated by SAL_{10}, TEM_{10} and GEO_{10}) and integrated values conditioned by the 2 depth limits: the median value of SAL, TEM and GEO from the surface to 70 m depth (indicated by SAL_{70}, TEM_{70} and $GEO_{70,}$) or the DTG limit (indicated by SAL_{DTG}, TEM_{DTG} and GEO_{DTG}). The 2D oceanographic variables (SSTG, DTG and MTG) and static variables were not modified by any vertical criteria.

To characterise the vertical domain, we explored the relationship between surface environmental conditions (both preyscape and oceanography) and integrated conditions above the DTG and down to 70 m depth. We calculated the non-parametric Spearman rank correlation coefficient between pairwise predictors.

2.3. Seabird detection functions

We applied multiple covariate distance sampling (Marques & Buckland 2004) to consider the effects of different observational (environmental) conditions affecting seabird detection probability. We developed detection functions based on both SOSH and GRSH sightings for the period 2013 to 2016 in good environmental conditions (i.e. Beaufort sea-state ≤5, wave height ≤2 m and overall medium and good conditions; García-Barón et al. 2019). Truncation distances for SOSHs and GRSHs were set to 400 and 600 m, respectively, to eliminate outliers and improve model fitting (Buckland et al. 2001). The elimination of the 5 to 10% of the most distant observations is a common procedure during the exploratory phase (Buckland et al. 1993). For each species, hazard-rate and half-normal models were fitted to perpendicular distances (Mannocci et al. 2014). We assessed the effect of different environmental conditions that could affect the detection probability (group size as a continuous variable, and year, Beaufort sea-state, wave height and cloud cover as factor variables; García-Barón et al. 2019). We selected the detection function that provided the lowest Akaike information criterion (AIC) value, informed by the p-value of the Cramér von Mises goodness-of-fit test (García-Barón et al. 2019). Then, the effective strip half-width (ESW) was calculated as the perpendicular distance in which the missing detections at lower distances were equal to the recorded detections at greater distances. ESW was used to estimate the effective sampled area ($L \times 2 \times$ ESW, where L is the length of the segment in km and ESW is in m). These analyses were conducted with the 'distance' package (Miller 2017).

2.4. Spatial abundance models

We developed seabird spatial abundance models to explore the effects of the 3D preyscapes (ANEJ, ANEA and PIL), the 3D (SAL, TEM and GEO) and 2D (DTG, MTG and SSTG) ocean dynamic environment and different static environmental variables (BAT, BATG, DSB and DCO) (Table 1).

2.4.1. Data processing

Before model development, each period of observation was divided into 10 km length segments of the same observation conditions (Lambert et al. 2017). The geographic position of the centroid of the segment was used to extract both dynamic preyscape and oceanographic conditions, as well as static variables.

2.4.2. General modelling framework

We used GAMs developed within the information theoretic approach using the 'mgcv' package (Wood 2011). The response variable (no. of seabirds segment^{-1}) was fitted following a negative binomial distribution (the over-dispersion parameter close to 1).

The effective sampled area was included as an offset. The smoothing splines were limited to a maximum of 3 degrees of freedom to capture non-linear associations without increasing the complexity of the functions towards unrealistic conclusions (Pérez-Jorge et al. 2015). Seabird observations were fitted to environmental data year by year, and not by combining all years.

2.4.3. Selecting the biologically meaningful depth range

We ran different set of GAMs including only preyscapes (ANEA, ANEJ and PIL), only 3D oceanographic predictors (SAL, TEM and GEO), and both together, at different depth ranges for each species. All sets of GAMs were compared based on AIC and explained deviance (ED). When models were within 2 points of AIC (AIC < 2), they were considered statistically equivalent (Williams et al. 2002). Models were first ordered by their AIC value, and between equivalent models the best model was chosen as the one with the highest ED.

2.4.4. Identifying non-collinear variables

Explanatory variables at selected depth ranges were standardised, and highly collinear pair-wise predictors were identified (Spearman rank correlation coefficient, $r_S \geq 0.5$) (Louzao et al. 2011). To keep the most explicative predictors, we compared the AIC values of the GAMs run with each predictor and selected the predictor yielding a model with a lower AIC value.

2.4.5. Model-averaging approach

GAMs were developed for a maximum of 4 predictors (Lambert et al. 2017) to avoid excessive complexity. Afterwards, models were developed for all possible combinations of predictors, and were ranked based on their AIC values and the Akaike weights using the 'MuMIn' package (Barton 2016). We obtained averaged coefficients and variance estimators from the models included in the 95% confidence set (i.e. including models in which the cumulative sum of Akaike weights was ≥0.95) (Burnham & Anderson 2002). The relative importance of predictors was measured by summing the Akaike weights for all models containing a specific predictor (Burnham & Anderson 2002). The ED of the model with the lowest AIC value was used to assess the explanatory power (Pérez-Jorge et al. 2015).

2.4.6. Mapping predictions

We mapped the most likely abundance predictions of pelagic seabirds over the standard grid. Whereas static variables were extracted once, dynamic variables were extracted for each year (i.e. every September survey). Averaged models were applied to descriptor grids to obtain spatial predictions of SOSH and GRSH densities (birds km^{-2}) every year.

Pelagic seabird abundance was calculated for each survey by summing the values resulting from multiplying the predicted density for each cell by the cell area (García-Barón et al. 2019). Furthermore, the 95% confidence interval was calculated assuming a positively skewed distribution of the predicted density (Buckland et al. 2001). Estimated abundances were relative (i.e. uncorrected) due to the absence of available data to correct for perception and availability bias for studied species or from alternative similar studies in the BoB.

3. RESULTS

3.1. Characterisation of the vertical domain

We analysed the correlation between preyscapes and oceanography between surface and depth-integrated conditions. ANEJ, ANEA and PIL were highly correlated at different depths, but correlations between surface and conditions above the DTG were higher for ANEA and PIL compared to those between the surface and conditions above 70 m depth (Table S4.1). Correlations between biomasses integrated between the surface and DTG or 70 m depth were high. Likewise, the correlation between oceanographic conditions at the surface and depth-integrated above the DTG or above 70 m depth yielded similar results (Table S4.2). Globally, shallower oceanographic conditions were more correlated with integrated oceanographic conditions above the DTG than above 70 m depth, even if the correlation was also high for SAL and GEO. In addition, correlations between both integrated oceanographic conditions at different vertical ranges were high. Due to the high correlation between each predictor estimated at different depth ranges, overall preyscape and oceanographic conditions were further described by conditions above the DTG (see Figs. 2 & 3).

3.2. 3D preyscapes

The spatial patterns of biomass of European anchovy showed a clear age-mediated spatial segregation, independent of the year. ANEJ were concentrated in the slope (both Spanish and French areas) and oceanic areas of the inner BoB, as well as over the French continental shelf (Fig. 2a–d). ANEA occupied a narrow band over the northern coastal French area (south of Brittany), the southern extension of which varied from year to year (Fig. 2e–h). The spatial extension of the main aggregation areas for the species and ages differed depending on the year considered. While ANEJ extended their distribution to the whole BoB in 2014 (including the oceanic area), ANEA were concentrated in specific hotspots over the French continental shelf in 2015, coinciding with the maximum total biomass.

In the case of PIL, the main aggregation areas overlapped with ANEA along a narrow band on the French coast (Fig. 2i–l). Biomasses of ANEA and PIL were highly correlated at all depth ranges considered (Table S4.1).

3.3. 3D oceanographic environment

The 3D oceanographic predictors showed important inter-annual variability. SAL_{DTG} showed a positive gradient from east to west, with lower values east of 4–5° W. The lowest SAL_{DTG} gradients were found in 2015, with higher values east of 4–5° W compared to the remaining years (Fig. 3a–d). TEM_{DTG} showed a positive gradient from north to south, with higher values south of 45° N, especially in the southeast corner of the BoB (Fig. 3e–h). Colder waters were also observed near the coast along the Spanish and French shelves, indicating the occurrence of upwelling events. However, inter-annual variability was reflected in lower overall TEM_{DTG} values in 2015 compared to the remaining years (Fig. 3e–h). In 2013 and 2016, a warm longitudinal band was identified over the Spanish slope, from 6–7° W to the French coast (Fig. 3e & h, respectively). Regarding GEO_{DTG}, density fields depicted an anticyclonic tendency (data not shown), with currents intensified over the shelf and slope (Fig. 3i–l). Different mesoscale structures were observed in each survey and the position and sizes of the eddy-like features were highly variable. 2015 was again the year showing a singular picture, with the less intense GEO_{DTG} values (Fig. 3k).

Regarding the 2D oceanographic variables, the DTG patterns observed were different between the analysed years (Fig. 4a–d). The lowest values for the DTG (values over the shelf and slope between 10 and 35 m) and MTG (values over the shelf and slope around 0.28°C m^{-1}) were observed in 2013 and 2016 (Fig. 4e–h), suggesting the weakest stratification. DTG was significantly deeper in 2015 (values between 20 and 50 m) and MTG was stronger compared to the remaining years (values over the shelf and slope around 0.36°C m^{-1}), although the surface heating of shelf waters at the SE of the domain was less intense (Fig. 3g). The highest SSTG values were located in shelf-break areas, especially in the southern BoB, which were especially high in 2013 (Fig. 4i–l).

3.4. Seabird sightings and detection functions

We observed a total of 360 SOSHs in 206 sightings (mean ± SD group size = 1.75 ± 2.74), while 1708 GRSHs were observed in 615 sightings (group size = 2.77 ± 6.52) for the period 2013 to 2016 (Fig. 1). After selecting data collected in 'good environmental conditions', we retained 183 and 552 sightings of SOSH and GRSH, respectively. After setting the truncation distance to 400 and 600 m, sightings were reduced to 171 and 523 (truncating at 6 and 5% of observations), respectively. For SOSHs, the detection function with the lowest AIC was the half normal with no covariates and it showed a non-significant Cramér von Mises goodness-of-fit test (Table S5.1, Fig. S5.1a,b). This detection function estimated an ESW of 195.45 m. For GRSHs, the hazard-rate detection model was selected with Beaufort sea-state as a covariate (Table S5.2, Fig. S5.1c,d). We estimated the corresponding ESW for GRSH at Beaufort sea-state 0, 1, 2, 3, 4 and 5 as 198, 278, 245, 332, 232 and 51 m, respectively.

3.5. Biologically meaningful vertical domain

Environmental conditions above the DTG and surface conditions led to models with lower AIC values for SOSHs and GRSHs, respectively (Table 2). Environmental conditions characterising the depth range 10–70 m were within the models with higher AIC values. Therefore, abundance patterns of each species were better explained by integrating preyscape and oceanographic conditions at different depth ranges.

3.6. Pelagic seabird 3D oceanographic habitat and abundance predictions

Among highly correlated predictors for SOSHs (Table S6.1), $ANEA_{DTG}$, SAL_{DTG}, BATG and DCO

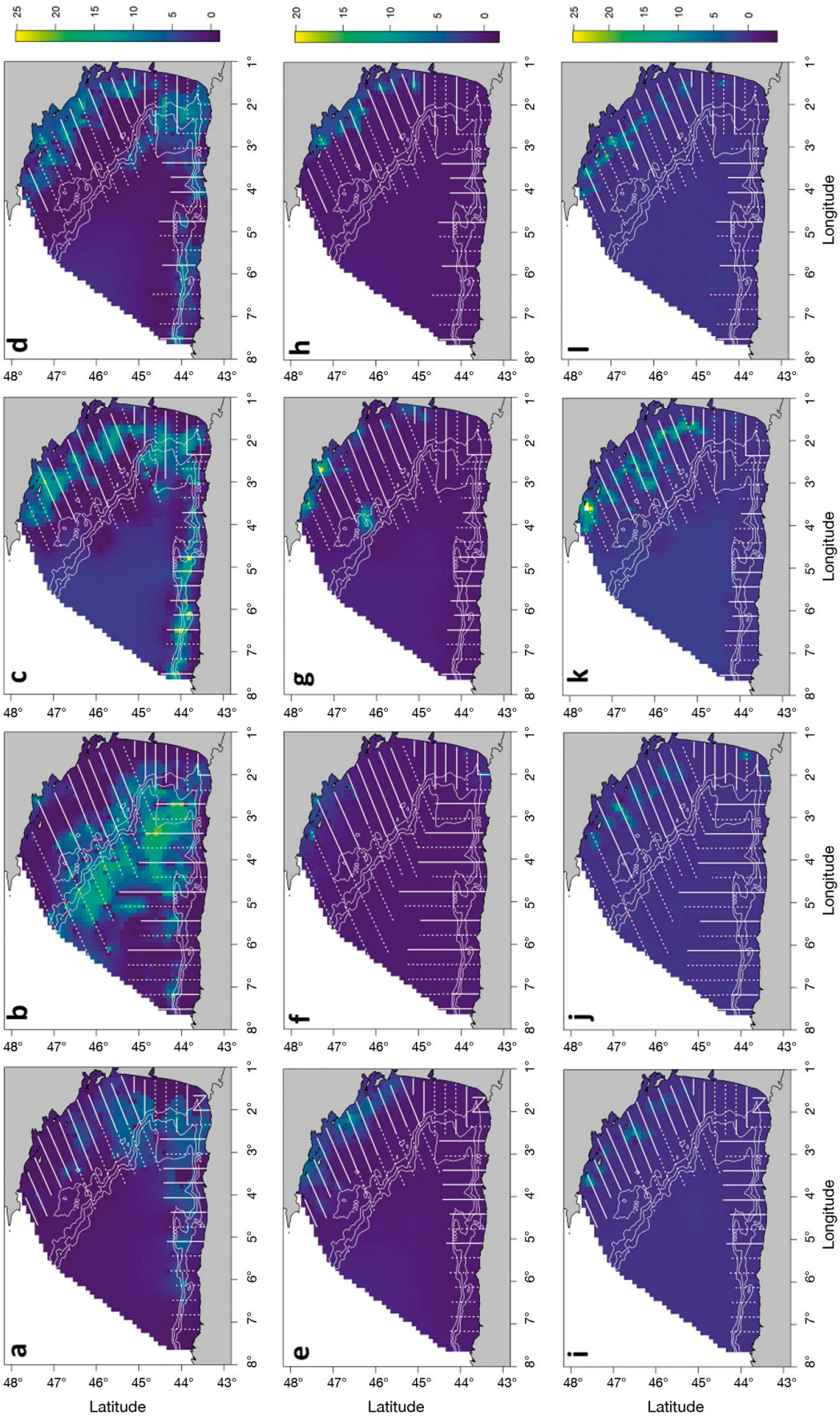

Fig. 2. The 3D preyscape represented by the spatial patterns of log-transformed biomass (tonnes) of (a–d) juveniles ($ANEJ_{DTG}$), and (e–h) adults of European anchovy ($ANEA_{DTG}$), as well as (i–l) European pilchard (PIL_{DTG}) summed from 5 m depth to the depth of maximum temperature gradient (DTG) during 2013–2016. White solid and dashed lines: annual effort coverage corresponding to the R/Vs 'Emma Bardán' and 'Ramón Margalef', respectively. Isobaths of 200, 1000 and 2000 m are outlined. Geographic references are indicated in Fig. 1

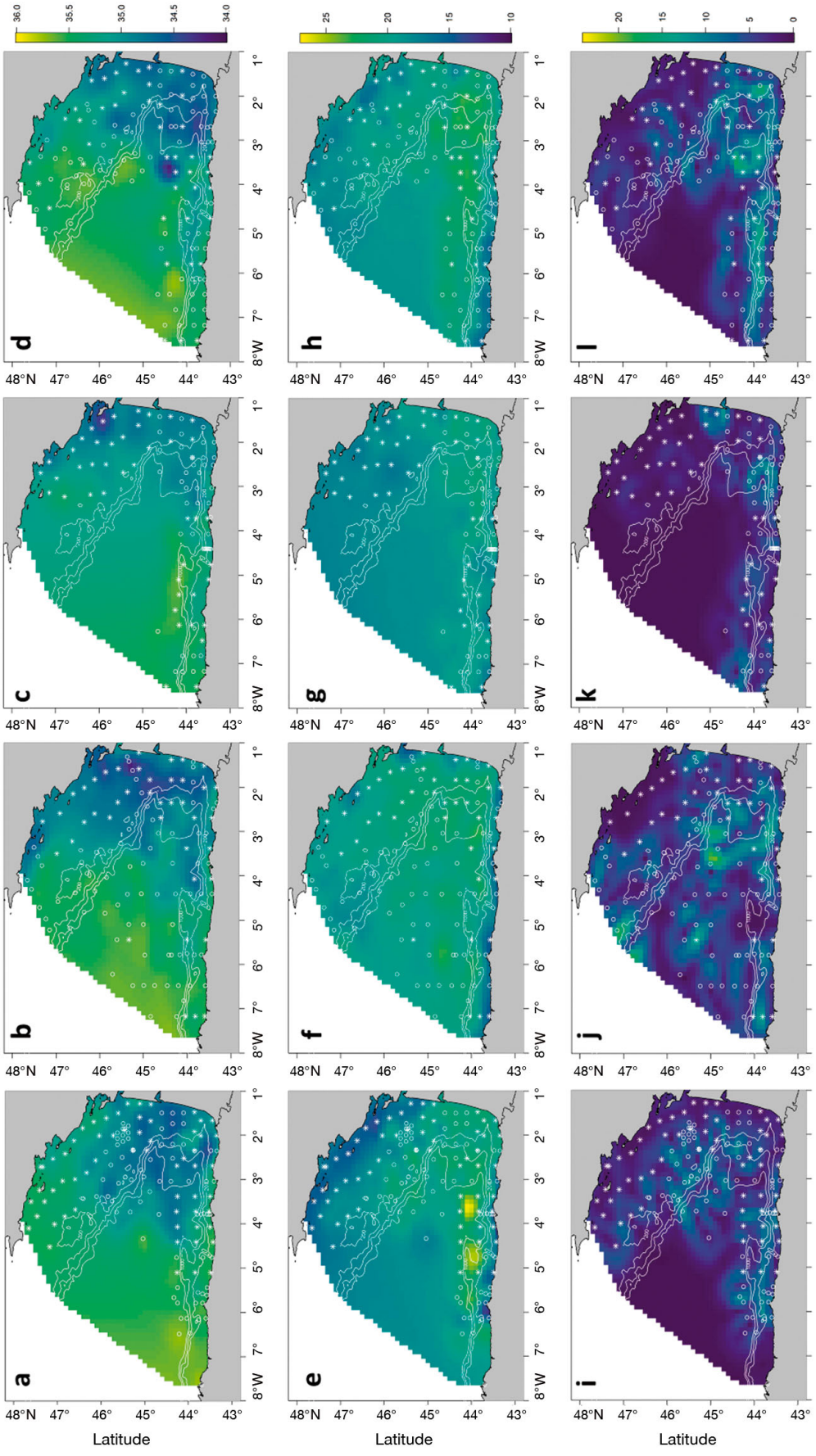

Fig. 3. The 3D oceanographic environment represented by median values of (a–d) salinity (SAL_{DTG}; values in psu), (e–h) temperature (TEM_{DTG}; values in °C) and (i–l) geostrophic velocity module (GEO_{DTG}; values in m s^{-1}) integrated between 10 m depth and the depth of maximum temperature gradient (DTG) during 2013–2016. Dots and stars: CTD casts performed by R/Vs 'Emma Bardán' and 'Ramón Margalef', respectively. Isobaths of 200, 1000 and 2000 m are outlined. Geographic references are indicated in Fig. 1

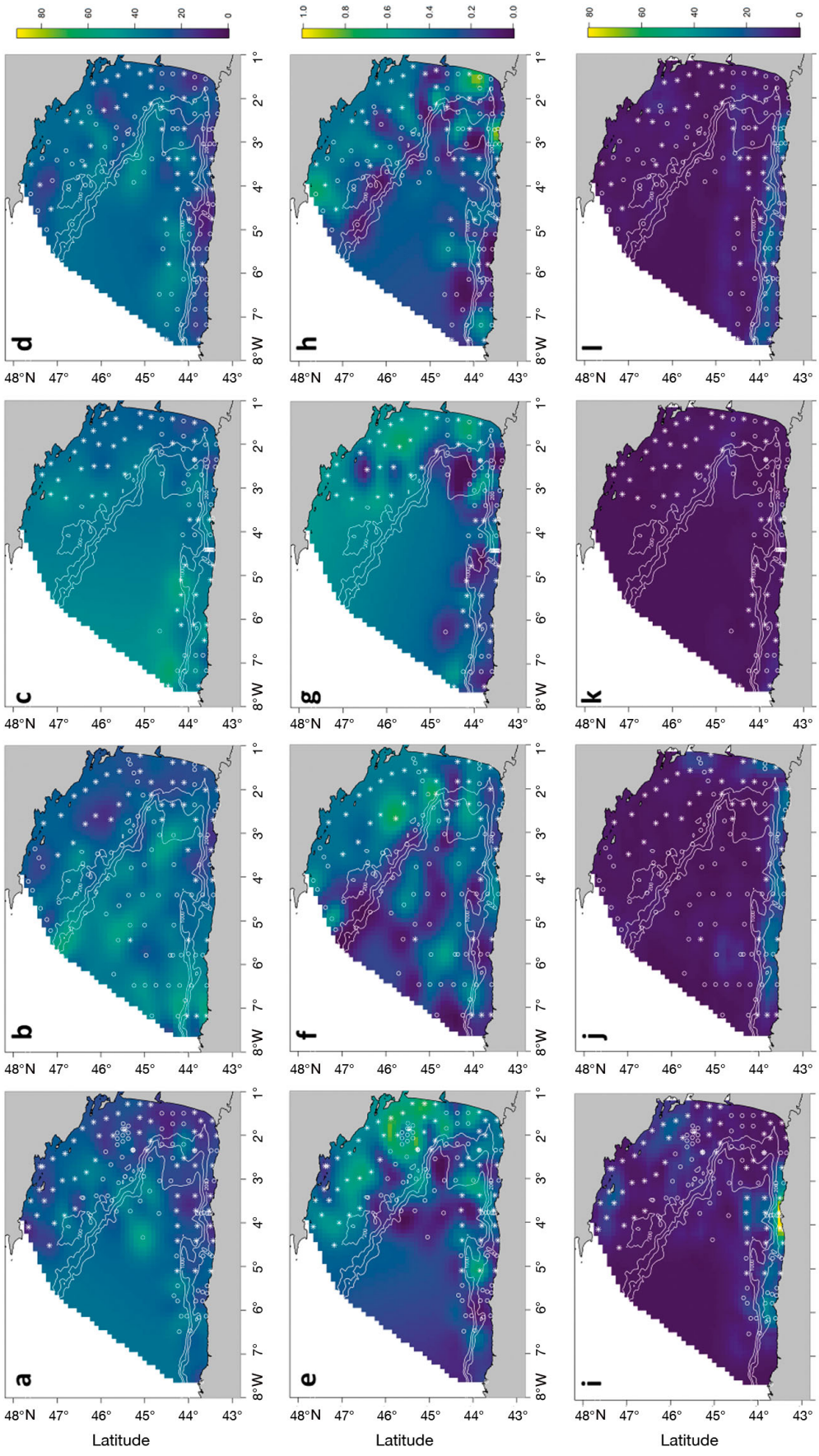

Fig. 4. The 2D oceanographic environment represented by (a–d) depth of maximum temperature gradient (DTG; values in m), (e–h) maximum temperature gradient (MTG; values in °C m^{-1}) and (i–l) sea surface temperature gradient (SSTG; non-dimensional) during 2013–2016. Dots and stars: CTD casts performed by R/Vs 'Emma Bardán' and 'Ramón Margalef', respectively. Isobaths of 200, 1000 and 2000 m are outlined. Geographic references are indicated in Fig. 1

Table 2. Generalized additive model output showing the ranking of candidate models based on their Akaike's information criterion (AIC) value by species (SOSH: sooty shearwater; GRSH: great shearwater), variable type (preyscape, oceanography or both types) and depth range considered (DTG: depth of maximum temperature gradient). Models are first ordered by the AIC value, and among equivalent models (i.e. AIC < 2) the best model is the one with the highest explained deviance (ED). Np: number of parameters. Selected models are in **bold**. See Table 1 for acronyms

Species	Data type	Depth range	Variables	Np	AIC	ED	AIC
SOSH	**Preyscape + oceanography**	**Above DTG**	**$ANEJ_{DTG}$ + $ANEJ_{DTG}$ + PIL_{DTG} + SAL_{DTG} + TEM_{DTG} + GEO_{DTG}**	**7**	**1239.323**	**0.127**	**1.007**
	Oceanography	Above DTG	SAL_{DTG} + TEM_{DTG} + GEO_{DTG}	4	1238.316	0.112	0
	Oceanography	Surface	SAL_{10} + TEM_{10} + GEO_{10}	4	1243.127	0.102	4.811
	Preyscape + oceanography	Surface	$ANEJ_{10}$ + $ANEJ_{10}$ + PIL_{10} + SAL_{10} + TEM_{10} + GEO_{10}	7	1246.042	0.109	7.726
	Preyscape + oceanography	10–70 m	$ANEJ_{70}$ + $ANEJ_{70}$ + PIL_{70} + $SAL_{70\ 0}$ + TEM_{70} + GEO_{7}	7	1246.303	0.118	7.987
	Oceanography	10–70 m	SAL_{70} + TEM_{70} + GEO_{70}	4	1254.377	0.072	16.061
	Preyscape	10–70 m	$ANEJ_{70}$ + $ANEJ_{70}$ + PIL_{70}	4	1258.349	0.057	20.033
	Preyscape	Above DTG	$ANEJ_{DTG}$ + $ANEJ_{DTG}$ + PIL_{DTG}	4	1261.321	0.054	23.005
	Preyscape	Surface	$ANEJ_{10}$ + $ANEJ_{10}$ + PIL_{10}	4	1265.063	0.044	26.747
GRSH	**Preyscape + oceanography**	**Surface**	**$ANEJ_{10}$ + $ANEJ_{10}$ + PIL_{10} + SAL_{10} + TEM_{10} + GEO_{10}**	**7**	**2154.028**	**0.122**	**0**
	Oceanography	Surface	SAL_{10} + TEM_{10} + GEO_{10}	4	2162.617	0.088	8.589
	Preyscape + oceanography	Above DTG	$ANEJ_{DTG}$ + $ANEJ_{DTG}$ + PIL_{DTG} + SAL_{DTG} + TEM_{DTG} + GEO_{DTG}	7	2164.189	0.101	10.161
	Oceanography	Above DTG	SAL_{DTG} + TEM_{DTG} + GEO_{DTG}	4	2166.962	0.079	12.934
	Preyscape	Surface	$ANEJ_{10}$ + $ANEJ_{10}$ + PIL_{10}	4	2189.718	0.033	35.69
	Preyscape + oceanography	10–70 m	$ANEJ_{70}$ + $ANEJ_{70}$ + PIL_{70} + SAL_{70} + TEM_{70} + GEO_{70}	7	2194.988	0.037	40.96
	Preyscape	10–70 m	$ANEJ_{70}$ + $ANEJ_{70}$ + PIL_{70}	4	2195.769	0.018	41.741
	Preyscape	Above DTG	$ANEJ_{DTG}$ + $ANEJ_{DTG}$ + PIL_{DTG}	4	2196.342	0.017	42.314
	Oceanography	10–70 m	SAL_{70} + TEM_{70} + GEO_{70}	4	2198.689	0.013	44.661

were the least explicative variables (results not shown) and they were not further considered. The 95% confidence set included 76 out of a total of 255 models. The model with the lowest AIC showed an ED of 16.7%. The main variables influencing SOSH abundance were BAT, SSTG, DTG and PIL_{DTG} (Fig. 5a). BAT influenced SOSH abundance negatively, with a decreasing negative trend up to 3000 m depth (Fig. 6a), followed by SSTG with an increasingly positively relationship (Fig. 6b). SOSH abundance showed a weak quadratic relationship with DTG, with higher abundances at approximately 35 m depth over both the Spanish and French shelves (Fig. 6c). Finally, SOSHs showed a slightly increasing relationship with increasing values of PIL_{DTG} (Fig. 6d). Globally, SOSH abundance was higher in

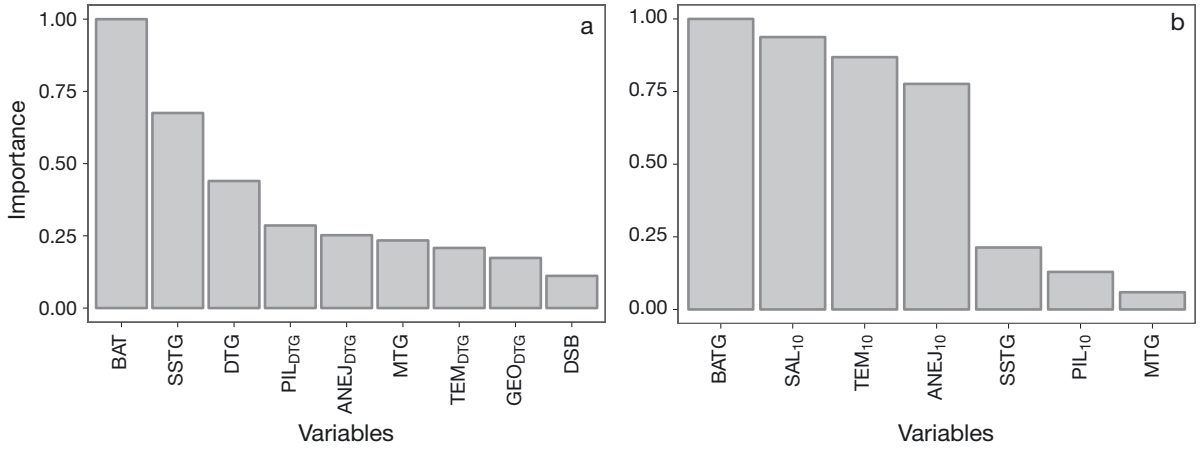

Fig. 5. Predictor importance in explaining (a) sooty and (b) great shearwater spatial abundance patterns. See Table 1 for acronyms

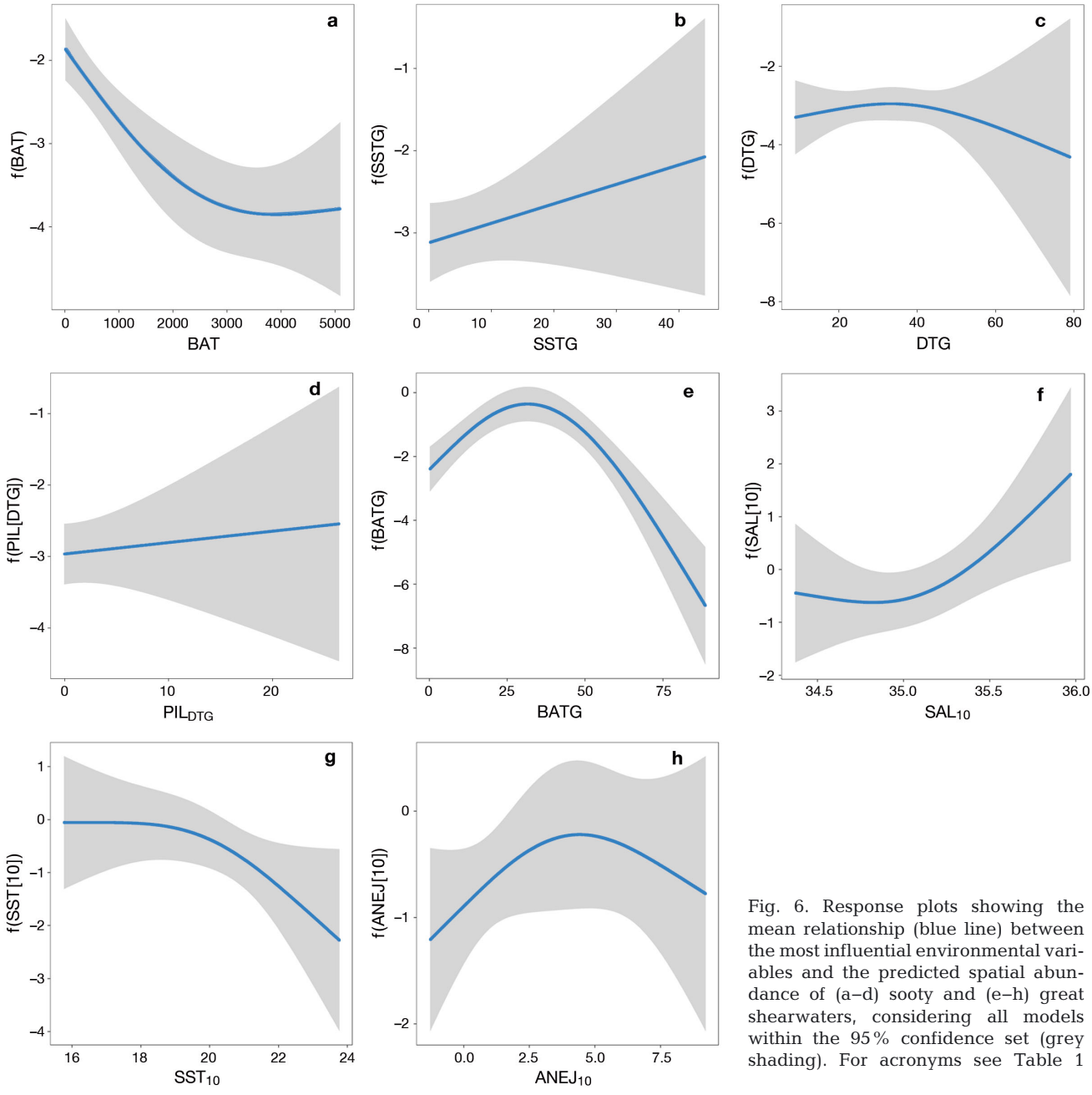

Fig. 6. Response plots showing the mean relationship (blue line) between the most influential environmental variables and the predicted spatial abundance of (a–d) sooty and (e–h) great shearwaters, considering all models within the 95% confidence set (grey shading). For acronyms see Table 1

shallow bathymetric ranges (i.e. over the continental shelf; Fig. S3.1a), in areas of higher spatial gradients of sea surface temperature (i.e. in the southern slope of the BoB; Fig. 4i–l), as well as in areas associated with medium DTG values (over shelf areas; Fig. 4a–d) of high PIL_{DTG} biomass (French coastal areas; Fig. 2i–l).

Among highly correlated predictors for GRSHs (Table S6.2), $ANEA_{10}$, BAT, DCO and DSB were the least explicative variables (results not shown) and they were removed. The 95% confidence set comprised 15 models out of a total of 255. The model with the lowest AIC showed an ED of 17.8%. The main variables driving the spatial abundance patterns of GRSHs were BATG, SAL_{10}, TEM_{10} and $ANEJ_{10}$ (Fig. 5b). Abundance of GRSHs showed a quadratic relationship with BATG, with maximum values at approximately 35% of BATG (Fig. 6e). SAL_{10} (ranging between 34 and 36 psu) and TEM_{10} (ranging between 16 and 24°C) influenced GRSH abundance positively (Fig. 6f) and negatively (Fig. 6g), respectively. Finally, intermediate $ANEJ_{10}$ values were related to higher GRSH abundance (Fig. 6h). In particular, GRSH abundance was higher at intermediate BATG values (i.e. corresponding to coastal and slope areas; Fig. S3.1b), in ar-

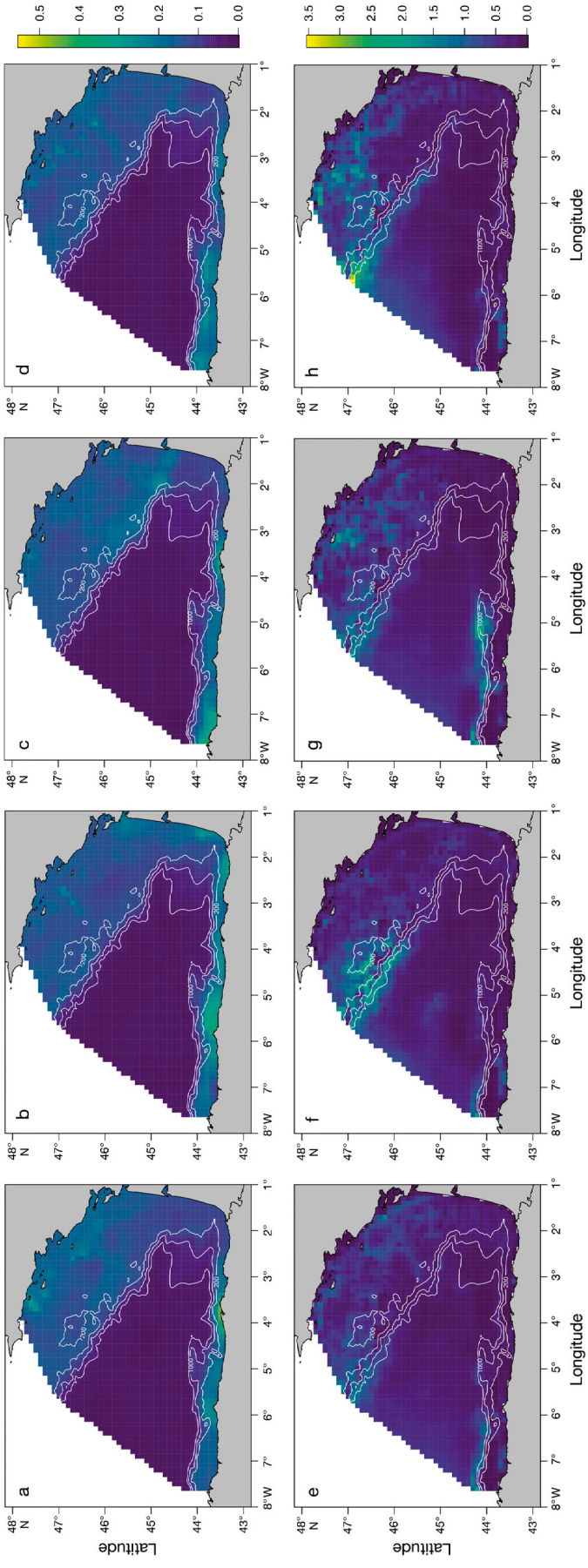

Fig. 7. Predicted spatial density of (a–d) sooty shearwaters and (e–h) great shearwaters for the 2013–2016 period during the JUVENA surveys. Predicted bird densities are represented in the colour scale bar; values range between 0–0.6 and 0–3.5 birds km^{-2} for both sooty and great shearwaters, respectively. Geographic references are indicated in Fig. 1

eas of higher SAL_{10} values (i.e. located in the southwestern shelf, slope and oceanic areas; Fig. S7.2a–d). In addition, GRSH abundance was higher in colder TEM_{10} occurring in the northern French continental shelf (Fig. S7.2e–h) and associated with areas of intermediate $ANEJ_{10}$ values (Fig. S7.1a–d).

Spatial abundance predictions showed the highest densities of SOSHs over both the Spanish and French continental shelves (Fig. 7a–d). Overall, higher densities were highlighted within specific marine areas around the main capes of the Spanish continental shelf (i.e. Estaca de Bares, Cabo Peñas, Cabo Ajo and Cabo Matxitxako, from west to east) and in specific coastal areas of the French continental shelf (e.g. the marine area surrounding the Belle-Île-en-Mer in south Brittany, and the area of influence of the Loire and Gironde rivers and the Arcachon Bay, from north to south). However, these areas showed high inter-annual variability and high-density areas were spread over both continental shelves. The lowest predicted relative densities were identified recurrently every year over the oceanic area of the BoB. Regarding GRSHs, spatial density predictions highlighted important areas in the French and Spanish continental slopes. These areas showed a high inter-annual variability over the Armorican slope (especially high in 2014 and 2016), and over the Cachucho area, an elongated near-shelf seamount (especially high in 2015). Less dense areas were located over the northern sector of the French continental shelf (Fig. 7e–h).

Predictions of relative density and abundance estimated that SOSHs were less abundant than GRSHs, showing an annual average of 3203 (95% CI: 1753–5748) and 12 380 (95% CI: 5797–28 152) birds, respectively (Table 3). Therefore, the SOSH:GRSH abundance ratio was almost 1:4. Averaged values of predicted relative densities yielded lower estimates for SOSHs compared to GRSHs (0.09 vs. 0.38 birds km^{-2}). Maximum density values were approximately 0.6 and 3.5 birds km^{-2} for SOSH and GRSH, respectively (Fig. 7).

Table 3. Abundance estimations of sooty (SOSH) and great shearwaters (GRSH) during JUVENA surveys for the 2013–2016 period. Animal density (D in ind. km^{-2}) and its coefficient of variation (CV_D), estimated abundance (N), its 95% confidence interval (95% CI_N) and its coefficient of variation (CV_N)

Species	Year	D	CV_D	N	95% CI_N	CV_N
SOSH	2013	0.09	0.3	3200	1810–5658	0.3
	2014	0.10	0.3	3250	1837–5748	0.3
	2015	0.09	0.3	3202	1785–5743	0.3
	2016	0.09	0.31	3162	1753–5702	0.31
GRSH	2013	0.35	0.35	11263	5797–21881	0.35
	2014	0.37	0.37	12160	6043–24466	0.37
	2015	0.39	0.42	12830	5847–28152	0.42
	2016	0.41	0.36	13269	6681–26354	0.36

4. DISCUSSION

This study illustrates the integration of predator observations, preyscapes and mesoscale oceanographic fields to assess the importance of foraging grounds for highly migratory pelagic predators. Determining migratory pathways of marine predators can have important implications for conservation strategies and climate change studies. Based on data collected during multidisciplinary oceanographic surveys, we characterised the 3D environment (preyscape plus oceanography) to explain abundance patterns of 2 highly migratory seabirds during their stage in the BoB. The JUVENA survey is featured by being a unique ecosystem-based survey that covers the oceanic area of the BoB. Based on our spatial modelling approach, we provide the first density and abundance values for SOSHs and GRSHs in the BoB.

Defining the 3D oceanographic habitats of marine species is challenging, owing to the difficulty in defining biologically meaningful spatial and vertical ranges at which they are able to integrate marine resources through the seascape. Here, we considered 3 different depth ranges, taking into account (1) surface conditions, (2) diving range (i.e. down to 70 m depth; Shaffer et al. 2009) and (3) accessibility of pelagic prey (Boyra et al. 2013, 2016). Our results highlighted species-specific biologically meaningful vertical domains. Whereas environmental conditions (both oceanography and preyscape) influencing prey accessibility (above the DTG) better explained SOSH observed abundance patterns, surface environmental conditions were better predictors of GRSH abundance patterns. Thus, each pelagic seabird species exploits the vertical habitat that they are able to reach: 70 and 20 m depth for SOSH and GRSH, respectively (Shaffer et al. 2009, Ronconi et al. 2010b). This is especially important for air-breathing predators (Benoit-Bird et al. 2013), since oceanographic covariates should characterise the vertical accessibility of forage fish to seabirds (Passuni et al. 2018). Therefore, both species integrate marine resources in different ways, even if prey and oceanographic conditions were highly correlated between the surface and above both the DTG and 70 m depth.

The 3D environments of both species were primarily influenced by different static, oceanographic and preyscape predictors, shaping a major 3D segregation. Overall, SOSHs were more abundant over the northern and southern continental shelves of the BoB, where this species could be regularly observed. Over the Spanish shelf, dense aggregations were located in areas of high SSTG (close to the main capes), probably influenced by summer coastal upwelling (Koutsikopoulos & Le Cann 1996). Over the French shelf, hotspots of the species were located in areas of low salinity associated with the discharge of the main rivers. The lowest densities were identified recurrently every year over the oceanic area of the BoB. In contrast, GRSH densities were higher in slope waters of the French (Armorican slope) and Spanish (southwestern slope) sectors, followed by less dense areas over the northern sector of the French continental shelf. Thus, this species could regularly be observed in the outer slope areas, characterised by high values of both bathymetric gradient and surface salinity. Over the Armorican slope, the generation of energetic internal waves has been reported (Serpette & Mazé 1989, Le Cann 1990, Pairaud et al. 2010). An increased variation in depth, which is also related to the generation of internal waves, has been linked to the higher probability of presence and abundance of 7 different species of seabirds and marine mammals in the North Sea (Scott et al. 2010). The formation of internal waves in those slope areas might promote an increase in primary production and aggregation of smaller prey items (Scott et al. 2010). Furthermore, internal waves may influence biological activity (plankton and small pelagic fish) at the sub-mesoscale level (100s of m to km), at a finer spatial scale than the JUVENA mesoscale survey (Bertrand et al. 2008, Grados et al. 2016). The effect of internal waves on mixing and the associated impact on seabirds in other areas of the BoB needs to be quantified and deserves further research.

Concerning preyscapes, abundance patterns of SOSHs and GRSHs were driven, to a certain extent, by the biomass of PIL and ANEJ, respectively. While

PIL were located mainly over the French coastal area, intermediate values of ANEJ biomass were located in the southern BoB and in the central French continental shelf (Boyra et al. 2013). The vertical distribution of the biomass of ANEJ show common depth ranges around 14 m depth (Boyra et al. 2013), shallower than the common depth of the PIL (e.g. Zwolinski et al. 2007). Depth ranges for these 2 small pelagic fishes are within the maximum diving depth recorded for the deep SOSH and shallow GRSH divers (Shaffer et al. 2009, Ronconi et al. 2010b). Therefore, this is the first study showing that early life stages of a small pelagic fish can drive the distribution patterns of seabirds in the BoB. However, the most important predictors were not the preyscapes, but the oceanographic ones (Torres et al. 2008). This could be related to (1) the wide spectrum of prey eaten by both species during the non-breeding period (krill, squid, sand lance and fishing discards) (Ronconi et al. 2010a), (2) the need to develop prey patch predictors (e.g. depth and local density of prey patches) in addition to prey biomass (Benoit-Bird et al. 2013), (3) the importance of considering the scale-dependence of predator–prey relationships (Rose & Leggett 1990, Fauchald et al. 2000) and (4) the problem of sampling scale in relation to ecosystem-process scales.

Spatial habitat segregation could be a mechanism to avoid inter-specific competition between 2 closely related species (Brown et al. 1981) that perform long-distance trans-equatorial migrations between the Northern and Southern Hemispheres (Huettmann & Diamond 2000, Shaffer et al. 2006, Hedd et al. 2012). This has been evidenced not only in the BoB (NE Atlantic), but also in their main non-breeding quarters in the NW Atlantic (Brown et al. 1981). In addition, observed spatial segregation could be partially explained by differences in forage fish depth distribution. In slope areas, where GRSHs concentrated, ANEJ are more abundant at shallower depths than in shelf areas, where they show a deeper vertical range (Boyra et al. 2016). Ultimately, both species differ in their foraging abilities, associated with bill morphology and underwater swimming adaptation (Brown et al. 1981). GRSHs might be adapted to obtain larger and tougher bodied prey such as squid (*Illex* spp.) and mackerel, whereas SOSHs feed preferentially upon euphausiids *Meganyctiphanes norvegica* and soft-bodied fish such as herring *Clupea harengus* (Brown et al. 1981).

The present study provides the first specific abundance values for both SOSH and GRSH in the BoB during September: 3203 SOSHs (95% CI: 1753–5748) and 12 380 GRSHs (95% CI: 5797–28 152), which vary slightly inter-annually. There are no alternative specific abundance values for SOSHs and GRSHs separately, but a large-sized shearwater group (pooling SOSH, GRSH and Cory's shearwaters) showed an abundance value of 31 980 individuals (95% CI: 21 324–48 776) for summer (mid-May to mid-August) (Pettex et al. 2017). Both studies (Pettex et al. 2017 and this study) provided similar figures and orders of magnitude, but differed in multiple factors such as different platforms (aerial vs. vessel-based surveys), methodologies (strip-transect vs. line-transect), surveyed months (mid-May to mid-August vs. September) and the time period considered (2012 vs. 2013–2016). Coastal counts during migration in the southwestern sector of the study area (Estaca de Bares) yielded an estimation of 54 501 SOSHs (range: 26 652–69 096) and 5898 GRSHs (range: 560–11 867) mainly in September–October in the northwestern tip of the Iberian Peninsula (Arcos et al. 2009, Sandoval et al. 2010). However, the arrival of these species is highly variable (Arcos et al. 2009), influenced by different climatic conditions leading the species into the BoB (Louzao et al. 2015). However, Louzao et al. (2015) provided higher numbers of GRSHs compared to SOSHs based on monthly at-sea surveys in the inner BoB, and the proportion of GRSHs to SOSHs was higher in the main stopover in the NW Atlantic Ocean (Huettmann & Diamond 2000). The ratio GRSH:SOSH of approximately 4:1 estimated in the present study falls within the observed ratio in the NW Atlantic, ranging from 3:1 to 30:1 (Huettmann & Diamond 2000).

Understanding the abundance patterns of highly migratory species and the underlying environmental drivers will assist in advancing current efforts to identify conservation targets in the pelagic realm (Game et al. 2009). We found inter-annual variability in both shearwater species' spatial abundance patterns, driven by annual oceanography and preyscapes. In the California Current system, SOSHs show an inter-annual variability in distribution and aggregation patterns within the shelf-slope area (Adams et al. 2012). However, persistent shearwater hotspots can be found, influenced by mesoscale oceanographic features (e.g. river plumes, oceanographic fronts or upwelling areas), since these areas support a large biomass of small pelagic fish (Adams et al. 2012). Within the non-breeding North Atlantic distribution, SOSHs wintering on the Newfoundland continental shelf are associated with persistent small pelagic fish hotspots (Davoren 2013). In the BoB, some of the oceanographic features influencing abun-

dance patterns of both shearwater species are predictable (e.g. coastal upwelling, area of influence of river plumes), occurring in similar spatial locations year after year (Llope et al. 2006). In addition, concentrations of small pelagic fish occur in the same overall areas every September (Boyra et al. 2013). Therefore, shearwater foraging locations could be spatially limited to guide conservation actions in the BoB.

The main objective of the JUVENA annual surveys is the assessment of ANEJ for predicting the strength of their recruitment to the adult stock the following year in the BoB (Boyra et al. 2013). Monitoring and management progress has recently been made due to the need for holistic management. Based on requirements established by frameworks such as the Marine Strategy Framework Directive (European Parliament and Council 2008), the JUVENA survey has widened its objectives to provide an integrative assessment of the BoB. The present study is a good example of such an effort by integrating not only other pelagic fish species but also marine megafauna monitoring and oceanographic characterisation in annual oceanographic surveys (Certain et al. 2011, Authier et al. 2018, Saavedra et al. 2018, García-Barón et al. 2019), in order to guide ecosystem-based management and conservation efforts. The spatial coverage of the JUVENA surveys (e.g. extended to the oceanic domain) is greater than any other monitoring scheme in the BoB (Massé & Uriarte 2016), but there are certain limitations caused by the use of 2 different research vessels. Predator observers are placed on only one of the vessels, and therefore a spatial modelling approach is necessary to obtain abundance estimations over the entire study area. In addition, a validation process is necessary to merge the data recorded from 2 different CTDs to obtain the oceanographic conditions of the survey. Despite these limitations, the present study illustrates the capabilities of annual oceanographic surveys in simultaneously characterising the 3D environment of different pelagic species, from plankton to marine predators (e.g. Certain et al. 2011).

In the present study, we have developed a methodological approach to identify biologically appropriate oceanographic and preyscape predictors to jointly consider both the spatial and vertical dimensions of oceanographic habitats, that can be applied to any marine species. Further research is necessary to develop integrative studies to understand the foraging strategies developed by predators in relation to prey patches (Benoit-Bird et al. 2013, Boyd et al. 2015). Fine-scale dedicated surveys would help understanding fine-scale interactions of marine megafauna with bio-physical variables, such as sub-surface chlorophyll and internal waves, by repeatedly surveying specific important marine areas (Scott et al. 2013). Other technologies, such as tracking devices, provide a complementary alternative to identify important marine areas for pelagic predators by providing continuous timescale information to evaluate seasonal, non-restricted at-sea distributions (Adams et al. 2012, Hedd et al. 2012, Pérez-Roda et al. 2017). The combination of at-sea surveys and tracking technologies provides complementary perspectives of the spatial ecology of pelagic predators (e.g. Louzao et al. 2009).

Acknowledgements. We thank to all crew and scientists participating in the JUVENA surveys on both the R/Vs 'Ramón Margalef' and 'Emma Bardán'. Special thanks to Unai Cotano (AZTI), Rafael González-Quirós (IEO) and Begoña Santos (IEO) for their support, as well as to Matthieu Authier (University of La Rochelle) for helping with the methodological development. The JUVENA survey was funded by the 'Viceconsejería de Agricultura, Pesca y Políticas Alimentarias – Departamento de Desarrollo Económico y Competitividad' of the Basque Government and the 'Secretaría General de Pesca, Ministerio de Agricultura, Alimentación y Medio Ambiente' of the Spanish Government. M.L. was funded by Juan de la Cierva (JCI-2010-07639) and a Ramón y Cajal (RYC-2012-09897) postdoctoral contracts of the Spanish Ministry of Economy, Industry and Competitiveness, whereas I.G.B. was supported by a PhD fellowship (FPI, BES-2014-070597) of the Spanish Ministry of Economy, Industry and Competitiveness. This study is a contribution to the CONPELHAB (PCIG09-GA-2011-293774) Marie Curie Career Integration grant project and the CHALLENGES (CTM2013-47032-R) project of the Spanish Ministry of Economy, Industry and Competitiveness. The comments of the Editor and 2 anonymous referees greatly improved the manuscript. Contribution number 899 from AZTI (Marine Research Division).

LITERATURE CITED

Adams J, MacLeod C, Suryan RM, Hyrenbach DK, Harvey JT (2012) Summer-time use of west coast US National Marine Sanctuaries by migrating sooty shearwaters (*Puffinus griseus*). Biol Conserv 156:105–116

Amante C, Eakins BW (2009) ETOPO1 1 arc-minute global relief model: procedures, data sources, and analysis. Tech Rep NESDIS NGDC-24. National Geophysical Data Center, NOAA, Boulder, CO

Arcos JM, Bécares J, Rodríguez B, Ruiz A (2009) Important areas for the conservation of seabirds in Spain. LIFE04NAT/ES/000049-Sociedad Española de Ornitología (SEO/BirdLife), Madrid

Authier M, Dorémus G, Van Canneyt O, Boubert JJ and others (2018) Exploring change in the relative abundance of marine megafauna in the Bay of Biscay, 2004–2016. Prog Oceanogr 166:159–167

Barrett RT (2002) Atlantic puffin *Fratercula arctica* and common guillemot *Uria aalge* chick diet and growth as indicators of fish stocks in the Barents Sea. Mar Ecol Prog Ser 230:275–287

Barton K (2016) MuMIn: multi-model inference. R package version 1.15.6

Benoit-Bird KJ, Battaile BC, Heppell SA, Hoover B and others (2013) Prey patch patterns predict habitat use by top marine predators with diverse foraging strategies. PLOS ONE 8:e53348

Bertrand A, Gerlotto F, Bertrand S, Gutiérrez M and others (2008) Schooling behaviour and environmental forcing in relation to anchoveta distribution: an analysis across multiple spatial scales. Prog Oceanogr 79:264–277

Bertrand S, Joo R, Arbulu Smet C, Tremblay Y, Barbraud C, Weimerskirch H (2012) Local depletion by a fishery can affect seabird foraging. J Appl Ecol 49:1168–1177

Block BA, Jonsen ID, Jorgensen SJ, Winship AJ and others (2011) Tracking apex marine predator movements in a dynamic ocean. Nature 475:86–90

Boyd C, Castillo R, Hunt GL, Punt AE, VanBlaricom GR, Weimerskirch H, Bertrand S (2015) Predictive modelling of habitat selection by marine predators with respect to the abundance and depth distribution of pelagic prey. J Anim Ecol 84:1575–1588

Boyra G, Martinez U, Cotano U, Santos M, Irigoien X, Uriarte A (2013) Acoustic surveys for juvenile anchovy in the Bay of Biscay: abundance estimate as an indicator of the next year's recruitment and spatial distribution patterns. ICES J Mar Sci 70:1354–1368

Boyra G, Peña M, Cotano U, Irigoien X, Rubio A, Nogueira E (2016) Spatial dynamics of juvenile anchovy in the Bay of Biscay. Fish Oceanogr 25:529–543

Brown RGB, Barker SP, Gaskin DE, Sandeman MR (1981) The foods of great and sooty shearwaters *Puffinus gravis* and *P. griseus* in eastern Canadian waters. Ibis 123:19–30

Buckland ST, Anderson DR, Burnham KP, Laake JL (1993) Distance sampling: estimation of biological populations. Chapman & Hall, New York, NY

Buckland ST, Anderson DR, Burnham KP, Laake JL, Borchers DL, Thomas L (2001) Introduction to distance sampling: estimating abundance of biological populations. Oxford University Press, New York, NY

Burnham KP, Anderson DR (2002) Model selection and multimodel inference: a practical information-theoretic approach. Springer-Verlag, New York, NY

Caballero A, Rubio A, Ruiz S, Le Cann B, Testor P, Mader J, Hernández C (2016) South-eastern Bay of Biscay eddy-induced anomalies and their effect on chlorophyll distribution. J Mar Syst 162:57–72

Certain G, Masse J, Van Canneyt O, Petitgas P, Doremus G, Santos M, Ridoux V (2011) Investigating the coupling between small pelagic fish and marine top predators using data collected from ecosystem-based surveys. Mar Ecol Prog Ser 422:23–39

Cox SL, Scott BE, Camphuysen CJ (2013) Combined spatial and tidal processes identify links between pelagic prey species and seabirds. Mar Ecol Prog Ser 479:203–221

Cury PM, Boyd IL, Bonhomeau S, Anker-Nilssen T and others (2011) Global seabird response to forage fish depletion—one-third for the birds. Science 334:1703–1706

Daunt F, Wanless S, Greenstreet SPR, Jensen H, Hamer KC, Harris MP (2008) The impact of the sandeel fishery closure on seabird food consumption, distribution, and productivity in the northwestern North Sea. Can J Fish Aquat Sci 65:362–381

Davoren GK (2013) Distribution of marine predator hotspots explained by persistent areas of prey. Mar Biol 160: 3043–3058

Doherty PD, Baxter JM, Gell FR, Godley BJ and others (2017) Long-term satellite tracking reveals variable seasonal migration strategies of basking sharks in the north-east Atlantic. Sci Rep 7:42837

European Parliament and Council (2008) Directive 2008/56/EC of the European Parliament and of the Council of 17 June 2008 establishing a framework for community action in the field of marine environmental policy. Off J Eur Union L 164:19–40

Fauchald P, Einar Erikstad K, Skarsfjord H (2000) Scale-dependent predator-prey interactions: the hierarchical spatial distribution of seabirds and prey. Ecology 81: 773–783

Fort J, Pettex E, Tremblay Y, Lorentsen SH and others (2012) Meta-population evidence of oriented chain migration in northern gannets (*Morus bassanus*). Front Ecol Environ 10:237–242

Fossette S, Hobson VJ, Girard C, Calmettes B, Gaspar P, Georges JY, Hays GC (2010) Spatio-temporal foraging patterns of a giant zooplanktivore, the leatherback turtle. J Mar Syst 81:225–234

Game ET, Grantham HS, Hobday AJ, Pressey RL and others (2009) Pelagic protected areas: the missing dimension in ocean conservation. Trends Ecol Evol 24: 360–369

García-Barón I, Authier M, Caballero A, Murcia JL, Vázquez JA, Santos MB, Louzao M (2019) Modelling the spatial abundance of a migratory predator: a call for transboundary marine protected areas. Divers Distrib doi: 10:1111/ddi.12877

Gomis D, Ruiz S, Pedder MA (2001) Diagnostic analysis of the 3D ageostrophic circulation from a multivariate spatial interpolation of CTD and ADCP data. Deep Sea Res I 48:269–295

Grados D, Bertrand A, Colas F, Echevin V and others (2016) Spatial and seasonal patterns of fine-scale to mesoscale upper ocean dynamics in an Eastern Boundary Current System. Prog Oceanogr 142:105–116

Hammond PS, Macleod K, Berggren P, Borchers DL and others (2013) Cetacean abundance and distribution in European Atlantic shelf waters to inform conservation and management. Biol Conserv 164:107–122

Hatch SA, Sanger GA (1992) Puffins as samples of juvenile pollock and other forage fish in the Gulf of Alaska. Mar Ecol Prog Ser 80:1–14

Hedd A, Montevecchi WA, Otley H, Phillips RA, Fifield DA (2012) Trans-equatorial migration and habitat use by sooty shearwaters *Puffinus griseus* from the South Atlantic during the nonbreeding season. Mar Ecol Prog Ser 449:277–290

Heinemann D (1981) A rangefinder for pelagic bird censusing. J Wildl Manag 45:489–493

Hiemstra PH, Pebesma EJ, Twenhöfel CJW, Heuvelink GBM (2009) Real-time automatic interpolation of ambient gamma dose rates from the Dutch radioactivity monitoring network. Comput Geosci 35:1711–1721

Hijmans RJ, van Etten J (2014) raster: geographic data analysis and modeling. R package version 2:15

Hobbs MJ, Brereton T, Weir C, Williams A (2003) Baseline monitoring data on Procellariformes (shearwaters) in the Bay of Biscay. Ornis Hung 12-13:115–125

Huettmann F, Diamond AW (2000) Seabird migration in the Canadian northwest Atlantic Ocean: moulting locations and movement patterns of immature birds. Can J Zool 78:624–647

Irigoien X, Fernandes JA, Grosjean P, Denis K, Albaina A, Santos M (2009) Spring zooplankton distribution in the Bay of Biscay from 1998 to 2006 in relation with anchovy recruitment. J Plankton Res 31:1–17

Koutsikopoulos C, Le Cann B (1996) Physical processes and hydrological structures related to the Bay of Biscay anchovy. Sci Mar 60:9–19

Lambert C, Laran S, David L, Dorémus G, Pettex E, Van Canneyt O, Ridoux V (2017) How does ocean seasonality drive habitat preferences of highly mobile top predators? Part II: The eastern North-Atlantic. Deep Sea Res II 141: 133–154

Lascelles B, Notarbartolo Di Sciara G, Agardy T, Cuttelod A and others (2014) Migratory marine species: their status, threats and conservation management needs. Aquat Conserv 24:111–127

Le Cann B (1990) Barotropic tidal dynamics of the Bay of Biscay shelf: observations, numerical modelling and physical interpretation. Cont Shelf Res 10:723–758

Lezama-Ochoa A, Boyra G, Goñi N, Arrizabalaga H, Bertrand A (2010) Investigating relationships between albacore tuna (*Thunnus alalunga*) CPUE and prey distribution in the Bay of Biscay. Prog Oceanogr 86:105–114

Llope M, Anadón R, Viesca L, Quevedo M, González-Quirós R, Stenseth NC (2006) Hydrography of the southern Bay of Biscay shelf-break region: integrating the multiscale physical variability over the period 1993–2003. J Geophys Res 111:C09021

Louzao M, Hyrenbach KD, Arcos JM, Abelló P, Gil de Sola L, Oro D (2006) Oceanographic habitat of an endangered Mediterranean procellariiform: implications for the design of marine protected areas. Ecol Appl 16:1683–1695

Louzao M, Bécares J, Rodríguez B, Hyrenbach KD, Ruiz A, Arcos JM (2009) Combining vessel-based surveys and tracking data to identify key marine areas for seabirds. Mar Ecol Prog Ser 391:183–197

Louzao M, Pinaud D, Péron C, Delord K, Wiegand T, Weimerskirch H (2011) Conserving pelagic habitats: seascape modelling of an oceanic top predator. J Appl Ecol 48:121–132

Louzao M, Afán I, Santos M, Brereton T (2015) The role of climate and food availability on driving decadal abundance patterns of highly migratory pelagic predators in the Bay of Biscay. Front Ecol Evol 3:90

Mannocci L, Laran S, Monestiez P, Dorémus G, Van Canneyt O, Watremez P, Ridoux V (2014) Predicting top predator habitats in the southwest Indian Ocean. Ecography 37:261–278

Marques FFC, Buckland ST (2004) Covariate models for the detection function. In: Buckland ST, Anderson DR, Burnham KP, Thomas L (eds) Advanced distance sampling. Oxford University Press, Oxford, p 31–47

Massé J (1996) Acoustic observations in the Bay of Biscay: schooling, vertical distribution, species assemblages and behaviour. Sci Mar 60 (Suppl 2):227–234

Massé J, Uriarte A (2016) Pelagic surveys series for sardine and anchovy in ICES Areas 8 and 9 (WGACEGG)—Towards an ecosystem approach. 2018. In: Massé J, Uriarte A, Angelico MM, Carrera P (eds) ICES-Cooperative Research Report 332, Copenhagen

Miller DL (2017) Distance: distance sampling detection function and abundance estimation. R package version 0.9.7. https://CRAN.R-project.org/package=Distance

Nur N, Jahncke J, Herzog MP, Howar J and others (2011) Where the wild things are: predicting hotspots of seabird aggregations in the California Current System. Ecol Appl 21:2241–2257

Nychka D, Furrer R, Paige J, Sain S (2017) fields: tools for spatial data. R package version 9.6. doi: 10.5065/D6W957CT

Pairaud IL, Auclair F, Marsaleix P, Lyard F, Pichon A (2010) Dynamics of the semi-diurnal and quarter-diurnal internal tides in the Bay of Biscay. Part 2: Baroclinic tides. Cont Shelf Res 30:253–269

Passuni G, Barbraud C, Chaigneau A, Bertrand A and others (2018) Long-term changes in the breeding seasonality of Peruvian seabirds and regime shifts in the Northern Humboldt Current System. Mar Ecol Prog Ser 597:231–242

Pérez-Jorge S, Pereira T, Corne C, Wijtten Z and others (2015) Can static habitat protection encompass critical areas for highly mobile marine top predators? Insights from coastal East Africa. PLOS ONE 10:e0133265

Pérez-Roda A, Delord K, Boué A, Arcos JM and others (2017) Identifying important Atlantic areas for the conservation of Balearic shearwaters: spatial overlap with conservation areas. Deep Sea Res II 141:285–293

Petitgas P, Masse J, Bourriau P, Beillois P and others (2006) Hydro-plankton characteristics and their relationship with sardine and anchovy distributions on the French shelf of the Bay of Biscay. Sci Mar 70 (Suppl 1):161–172

Pettex E, Laran S, Authier M, Blanck A and others (2017) Using large scale surveys to investigate seasonal variations in seabird distribution and abundance. Part II: The Bay of Biscay and the English Channel. Deep Sea Res II 141:86–101

Phillips EM, Horne JK, Zamon JE (2017) Predator–prey interactions influenced by a dynamic river plume. Can J Fish Aquat Sci 74:1375–1390

Regular PM, Hedd A, Montevecchi WA (2013) Must marine predators always follow scaling laws? Memory guides the foraging decisions of a pursuit-diving seabird. Anim Behav 86:545–552

Ronconi RA, Burger AE (2009) Estimating seabird densities from vessel transects: distance sampling and implications for strip transects. Aquat Biol 4:297–309

Ronconi RA, Koopman HN, McKinstry CAE, Wong SNP, Westgate AJ (2010a) Inter-annual variability in diet of non-breeding pelagic seabirds *Puffinus* spp. at migratory staging areas: evidence from stable isotopes and fatty acids. Mar Ecol Prog Ser 419:267–282

Ronconi RA, Ryan PG, Ropert-Coudert Y (2010b) Diving of great shearwaters (*Puffinus gravis*) in cold and warm water regions of the South Atlantic Ocean. PLOS ONE 5: e15508

Rose GA, Leggett WC (1990) The importance of scale to predator prey spatial correlations: an example of Atlantic fishes. Ecology 71:33–43

Rubio A, Gomis D, Jordà G, Espino M (2009) Estimating geostrophic and total velocities from CTD and ADCP data: intercomparison of different methods. J Mar Syst 77:61–76

Saavedra C, Gerrodette T, Louzao M, Valeiras J and others (2018) Assessing the environmental status of the short-beaked common dolphin (*Delphinus delphis*) in northwestern Spanish waters using abundance trends and safe removal limits. Prog Oceanogr 166:66–75

Sandoval A, Hevia R, Fernández D, Valderas A (2010) Boletín de la Estación Ornitológica de Estaca de Bares. Número 2 - Año 2009. Dirección Xeral de Conservación da Natureza, Consellería do Medio Rural da Xunta de

Galicia/TERRANOVA Interpretación y Gestión Ambiental, S.L.

Santos MB, González-Quirós R, Riveiro I, Iglesias M, Louzao M, Pierce GJ (2013) Characterization of the pelagic fish community of the north-western and northern Spanish shelf waters. J Fish Biol 83:716–738

Scott BE, Sharples J, Ross ON, Wang J, Pierce GJ, Camphuysen CJ (2010) Sub-surface hotspots in shallow seas: fine-scale limited locations of top predator foraging habitat indicated by tidal mixing and sub-surface chlorophyll. Mar Ecol Prog Ser 408:207–226

Scott BE, Webb A, Palmer MR, Embling CB, Sharples J (2013) Fine scale bio-physical oceanographic characteristics predict the foraging occurrence of contrasting seabird species; gannet (*Morus bassanus*) and storm petrel (*Hydrobates pelagicus*). Prog Oceanogr 117: 118–129

Serpette A, Mazé R (1989) Internal tides in the Bay of Biscay: a two-dimensional model. Cont Shelf Res 9:795–821

Shaffer SA, Tremblay Y, Weimerskirch H, Scott D and others (2006) Migratory shearwaters integrate oceanic resources across the Pacific Ocean in an endless summer. Proc Natl Acad Sci USA 103:12799–12802

Shaffer S, Weimerskirch H, Scott D, Pinaud D and others (2009) Spatiotemporal habitat use by breeding sooty shearwaters *Puffinus griseus.* Mar Ecol Prog Ser 391: 209–220

Simmonds J, MacLennan D (2005) Fishery acoustic theory and practice. Blackwell Scientific Publications, Oxford

Stenhouse IJ, Egevang C, Phillips RA (2012) Trans-equatorial migration, staging sites and wintering area of Sabine's gulls *Larus sabini* in the Atlantic Ocean. Ibis 154:42–51

Sydeman WJ, Thompson SA, Anker-Nilssen T, Arimitsu M and others (2017) Best practices for assessing forage fish fisheries-seabird resource competition. Fish Res 194: 209–221

Thackeray SJ, Sparks TH, Frederiksen M, Burthe S and others (2010) Trophic level asynchrony in rates of phenological change for marine, freshwater and terrestrial environments. Glob Change Biol 16:3304–3313

Thaxter CB, Daunt F, Grémillet D, Harris MP and others (2013) Modelling the effects of prey size and distribution on prey capture rates of two sympatric marine predators. PLOS ONE 8:e79915

Torres LG, Read AJ, Halpin P (2008) Fine-scale habitat modeling of a top marine predator: Do prey data improve predictive capacity? Ecol Appl 18:1702–1717

Williams BK, Nichols JD, Conroy MJ (2002) Analysis and management of animal populations: modeling, estimation, and decision making. Academic Press, San Diego, CA

Wood SN (2011) Fast stable restricted maximum likelihood and marginal likelihood estimation of semiparametric generalized linear models. J R Stat Soc B 73:3–36

Zwolinski J, Morais A, Marques V, Stratoudakis Y, Fernandes PG (2007) Diel variation in the vertical distribution and schooling behaviour of sardine (*Sardina pilchardus*) off Portugal. ICES J Mar Sci 64:963–972

Editorial responsibility: Arnaud Bertrand (Guest Editor), Sète, France

Submitted: September 18, 2017; Accepted: December 3, 2018
Proofs received from author(s): January 21, 2019